The CoAlCeO Mixed Oxide: An Alternative to Palladium-Based Catalysts for Total Oxidation of Industrial VOCs

Julien Brunet, Eric Genty, Cédric Barroo, Fabrice Cazier, Christophe Poupin, Stéphane Siffert, Diane Thomas, Guy de Weireld, Thierry Visart de Bocarmé, Renaud Cousin

catalysts

MDPI

Article

The CoAlCeO Mixed Oxide: An Alternative to Palladium-Based Catalysts for Total Oxidation of Industrial VOCs

Julien Brunet [1,*], Eric Genty [1,2], Cédric Barroo [2], Fabrice Cazier [3], Christophe Poupin [1], Stéphane Siffert [1], Diane Thomas [4], Guy De Weireld [4], Thierry Visart de Bocarmé [2] and Renaud Cousin [1,*]

1 Unité de Chimie Environnementale et Interactions sur le Vivant, Université du Littoral Côté d'Opale, MREI1—145 Avenue Maurice Schumann, 59140 Dunkerque, France; eric.genty@ulb.ac.be (E.G.); Christophe.Poupin@univ-littoral.fr (C.P.); stephane.siffert@univ-littoral.fr (S.S.)
2 Chemical Physics of Materials and Catalysis, Université Libre de Bruxelles, Faculty of Sciences, Campus Plaine CP 243, 1050 Brussels, Belgium; cbarroo@ulb.ac.be (C.B.); Thierry.Visart.de.Bocarme@ulb.ac.be (T.V.d.B.)
3 Centre Commun de Mesures, Université du Littoral Côté d'Opale, MREI1—145 Avenue Maurice Schumann, 59140 Dunkerque, France; cazier@univ-littoral.fr
4 Faculté Polytechnique de Mons, Université de Mons, 20 Place du Parc, B-7000 Mons, Belgium; Diane.THOMAS@umons.ac.be (D.T.); Guy.DEWEIRELD@umons.ac.be (G.D.W.)
* Correspondence: julien.brunet@univ-littoral.fr (J.B.); renaud.cousin@univ-littoral.fr (R.C.)

Received: 15 December 2017; Accepted: 1 February 2018; Published: 6 February 2018

Abstract: Catalytic total oxidation is an effective technique for the treatment of industrial VOCs principally resulting from industrial processes using solvents, and usually containing mono-aromatics (BTEX) and oxygenated compounds (acetone, ethanol, butanone). The catalytic total oxidation of VOCs on noble metal materials is effective. However, the cost of catalysts is a main obstacle for the industrial application of these VOC removal processes. Therefore, the aim of this work is to propose an alternative material to palladium-based catalysts (which are suitable for VOCs' total oxidation): a mixed oxide synthesized in the hydrotalcite way, namely CoAlCeO. This material was compared to four catalytic materials containing palladium, selected according to the literature: Pd/α-Al_2O_3, Pd/HY, Pd/CeO_2 and Pd/γAl_2O_3. These materials have been studied for the total oxidation of toluene, butanone, and VOCs mixtures. Catalysts' performances were compared, taking into account the oxidation byproducts emitted from the process. This work highlight that the CoAlCeO catalyst presents better efficiency than Pd-based materials for the total oxidation of a VOCs mixture.

Keywords: mixed oxide catalyst; VOCs; byproducts; BTEX; catalytic total oxidation; CoAlCeO

1. Introduction

Volatile organic compounds (VOCs) are known as one of the major contributors to atmospheric pollution. Their anthropic release is particularly significant in industrialized areas and has noxious consequences for health, environment, and construction materials. The majority of VOC emissions originates from solvents used in several industrial sectors (paints, varnishes, lacquers, inks, adhesives, glues, etc.). A significant part of these solvents is composed of mono-aromatic compounds, particularly BTEX (benzene, toluene, ethylbenzene, and xylenes). The other part of these solvents is represented by oxygenated compounds, such as butanone (or methyl ethyl ketone (MEK)) which is a common oxygenated solvent, since it is a less toxic substitute for alcohols (methanol, ethanol) and acetone. Butanone and BTEX are also widely used in mixtures as solvent for lacquers, inks, and coatings for application to metal surfaces.

An effective method for the treatment of industrial VOC emissions is their catalytic oxidation which is a cost-effective and an ecological alternative to thermal oxidation, with similar efficiency. Studies of the BTEX oxidation, especially toluene, have been widely reported in the literature [1–7]. Oxidation of butanone is also well known in the literature, although the number of studies is more restricted [7–12]. However, studies of the catalytic oxidation of BTEX and oxygenated compounds in mixture are very limited, even though this is an important step towards industrial applications. Concerning the oxidation of VOCs mixture, the authors generally observe inhibition phenomena [7,13–18] that are either caused by competition between molecules, or at the level of the adsorption step to the surface of the catalyst during the mechanism of oxidation (a reaction with chemisorbed oxygen or lattice oxygen). These interactions depend on the VOC conformation and polarity, but also on the nature of the catalytic material. Furthermore, some molecules can react directly in the gas phase in contact with lattice oxygen, while others must be adsorbed to the catalyst surface before being oxidized. Oxidation of the latter will be strongly inhibited in favor of the former due to more favorable kinetics. Similarly, the oxidation of several compounds that need to be adsorbed on the catalyst will lead to adsorption competition.

In this work, a new and original approach to the total oxidation of VOCs is presented. Indeed, the catalytic oxidation of toluene and butanone alone or in mixture is presented for several materials, with a focus on the formed byproducts. Toluene and butanone have been chosen in accordance with effluents from industrial processes using lacquers, inks, and varnishes for application to metal surfaces. For this, various materials had been screened in order to find the most suitable catalyst for the catalytic treatment of VOCs from these industries. Firstly, palladium-based catalysts have been selected: Pd/HY, Pd/CeO_2, $Pd/\alpha\text{-}Al_2O_3$, and a commercial $Pd/\gamma\text{-}Al_2O_3$. Palladium generally shows an equivalent or superior activity to platinum for the total oxidation of aromatic compounds [15,19,20]. Moreover, Pd is more resistant than Pt to sintering, the formation of volatile metal species, and poisoning by chlorine, water, and carbon monoxide [16,21,22]. Thus, these materials are particularly suited for the oxidation of VOC, especially BTEX. They have already been presented in a previous study on the total oxidation of toluene [3]. Secondly, as an alternative to the use of precious metals-based materials, our research group has conducted several studies to develop efficient transition metal oxides for environmental catalytic applications. Indeed, the catalyst cost is an important limitation for the industrial application of VOC catalytic oxidation processes. These studies led to the development of a Co–Al–Ce mixed oxide, denoted CoAlCeO, which reveals promising results concerning the oxidation of toluene [23]. Therefore, in this framework, these materials were compared for the total oxidation of toluene, butanone, and finally VOC mixtures (MEK/toluene and industrial mixtures).

2. Results

2.1. Catalysts Characterization

The catalysts used in this study were first characterized to obtain information on the specific surface area, the Pd content, the dispersion and particle size, as well as the molar ratio in the case of the CoAlCeO catalyst. These details are reported in Table 1. Furthermore, the X-ray diffraction patterns of the different materials are presented in Figure 1.

Table 1. Characterization of the studied catalytic materials.

	$Pd/\alpha\text{-}Al_2O_3$	**Pd/HY**	**Pd/CeO_2**	**$Pd/\gamma\text{-}Al_2O_3$**	**CoAlCeO**
Specific surface area ($m^2 \cdot g^{-1}$)	1	900	93	252	108
Palladium content (wt %)	0.48	0.46	0.40	0.40	N.A.
Palladium dispersion (%)	13.8	62.7	34.5	26.4	N.A.
Palladium particle size (nm)	8.1	1.8	3.2	4.3	N.A.
Co/Al/Ce Experimental molar ratio	N.A.	N.A.	N.A.	N.A.	6/1.1/0.8

Regarding palladium-based materials, different diffractograms show only the presence of the support, a sign that no supported palladium phase was detected. Nevertheless, the elementary analysis confirms the presence of palladium in several materials with relatively good depositionrates: this indicates that the palladium is deposited in the form of small nanoparticles whose size is lower than the detection limit of the diffractometer. This hypothesis was confirmed by hydrogen chemisorption measurements that indicate particle sizes between 1.8 and 8.1 nm. Concerning the $Co_6Al_{1.2}Ce_{0.8}O_x$ material, denominated CoAlCeO, the diffractogram reveals X-ray patterns characteristic of spinel-type oxides $M^{II}M^{III}{}_2O_4$ [24–26] corresponding to Co_3O_4, $CoAl_2O_4$ or Co_2AlO_4. In addition to the spinel phase, the diffraction pattern also showed the presence of a ceria phase (CeO_2) (Figure 1).

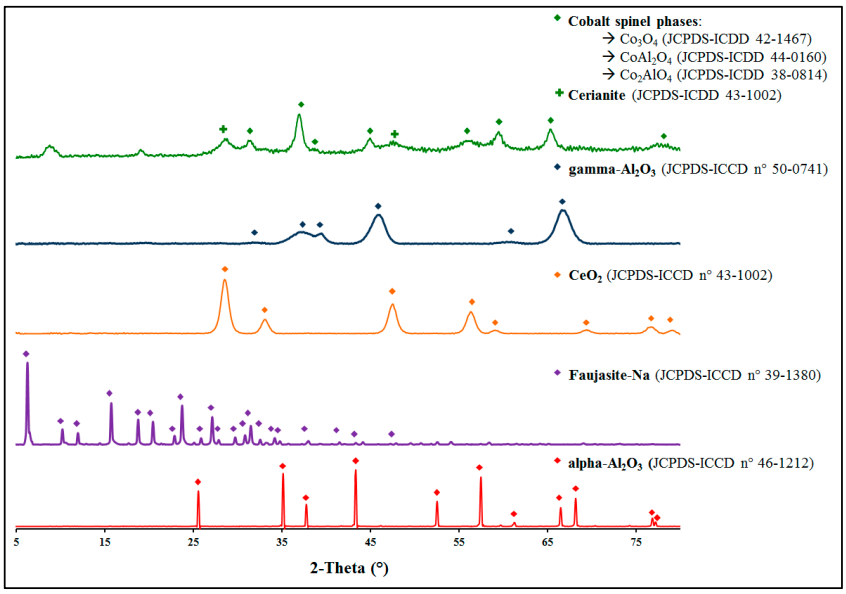

Figure 1. X-ray diffraction patterns of the catalysts.

2.2. Toluene Oxidation

As a first set of experiments, the materials of interest were used to investigate the total oxidation of toluene, and the light-off curves obtained are shown in Figure 2 for all materials.

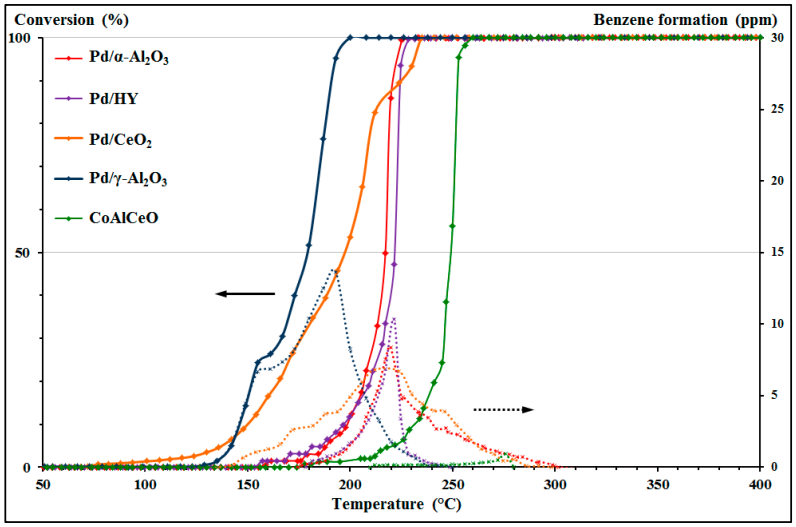

Figure 2. Toluene conversion (solid arrow and lines) and benzene formation (dashed arrow and lines) versus temperature for each catalyst.

The light-off curves of Pd-based catalysts have been presented in a previous study (Pd/α-Al_2O_3, Pd/HY, Pd/CeO_2 and Pd/γ-Al_2O_3) [3]. T_{50} and T_{100} are defined as the temperature when 50% and 100% conversion, respectively, was observed. These values of T_{50} and T_{100} for toluene oxidation are reported in Table 2. The test conducted with pure SiC shows only a slight toluene conversion from 360 °C, with a maximum of 5% at 400 °C. This can be explained by a thermal decomposition. Indeed, the test performed under the same conditions with the empty reactor leads to the same result. The results show that the mixed oxide has a lower performance than palladium-based catalysts. However, with a T_{50} value of 249 °C, the CoAlCeO material shows excellent activity for the toluene total oxidation. Moreover, in view of the activity values (A) in Table 2, it is possible to observe that the mixed oxide has a similar activity to that of Pd/CeO_2 and Pd/γ-Al_2O_3 catalysts, highlighting the possibility of such catalysts replacing Pd-based materials in the VOCs removal processes.

Table 2. T_{50} and T_{100} of catalysts for toluene catalytic oxidation and parameters characterizing the emission profiles of benzene.

Catalyst	T_{50} (°C)	T_{100} (°C)	A (mol/(m^2·h))	Q_{max} (ppm)	T_f (°C)	P (°C)
Pd/α-Al_2O_3	218	233	2.84×10^{-7}	8	300	67
Pd/HY	222	242	3.18×10^{-10}	10	249	7
Pd/CeO_2	197	235	3.34×10^{-9}	7	298	63
Pd/γ-Al_2O_3	179	200	1.27×10^{-9}	14	244	44
CoAlCeO	249	260	2.45×10^{-9}	0.9	280	20

As for palladium-based materials, the CoAlCeO mixed oxide was investigated regarding its properties to form byproducts, in particular benzene. In addition to the toluene conversion, Figure 2 shows the benzene emission profiles (as dashed lines) as a function of toluene conversion (solid lines) and temperature. The results show that the four palladium-based catalysts present similar emission profiles, with a maximum value at around 10 ppm. By contrast, the emission profile of the CoAlCeO mixed oxide revealed a maximum value of less than 1 ppm, namely an order of magnitude lower as compared to the other catalysts. In order to compare the benzene emissions of each material, the methodology presented in a previous study has been used [3], where the emission profiles are characterized by seven parameters. However, only the most relevant parameters are presented in this paper:

Q_{max}: maximum quantity emitted observed of the considered byproduct (ppm);
T_f: temperature at which the byproduct is totally oxidized (°C);
P: persistence of byproduct, corresponding to the difference between T_f and T_{100} (°C).

Table 2 reports the values of Q_{max}, T_f and P. Regarding Pd/α-Al_2O_3, Pd/HY, Pd/CeO_2, and Pd/γ-Al_2O_3 catalysts, the Q_{max} values present a maximum amount of emitted benzene between 7 and 14 ppm. These values are relatively low as compared to the concentration of oxidized toluene. However, by taking into account the toxicity of this compound and its strict regulations, these values remain important. On the contrary, the CoAlCeO catalyst presents the lowest emissions with a Q_{max} value of 0.9 ppm. Concerning the P values, they are positive (on average 40 °C), which clearly indicates that benzene is not fully oxidized when the toluene total oxidation (T_{100}) is reached. Therefore, this shows that benzene is a crucial limitation to the catalytic process of toluene oxidation: it is then necessary to consider this byproduct in order to set the working temperature of the process so as to oxidize all organic compounds. Both materials Pd/HY and CoAlCeO stand with the lowest P values of 7 and 20 °C respectively, sign of their improved performance for benzene oxidation.

To achieve real VOCs total oxidation, the working temperature must be set assuming the total oxidation of the reactant and its byproducts. This fact is supported by the toxic and regulatory aspects related to benzene. Therefore, the classification of the catalysts by their performance must be reassessed. Subsequently, according to the T_{50} and T_{100}, the ranking is as follows, from the most efficient to the least

efficient: $Pd/\gamma\text{-}Al_2O_3 > Pd/\alpha\text{-}Al_2O_3 > Pd/CeO_2 > Pd/HY > CoAlCeO$. Considering the emissions of benzene, as T_f, this classification may be reviewed as follows: $Pd/\gamma\text{-}Al_2O_3 > Pd/HY > CoAlCeO > Pd/CeO_2 > Pd/\alpha\text{-}Al_2O_3$. The difference between the T_{100} value of $Pd/\gamma\text{-}Al_2O_3$ and Pd/HY catalysts is then reduced from 42 °C to 5 °C by considering the T_f value corresponding to the temperature at which toluene is totally converted. Thus, the performances of these two materials are very close. Moreover, if the CoAlCeO catalyst exhibits lower performance considering only T_{50} and T_{100} values, it is by far the lowest benzene emitter and consequently, accounting for this point, CoAlCeO is among the best catalysts for toluene oxidation.

2.3. Butanone Oxidation

After analyzing the efficiency of the different catalytic materials for toluene oxidation, these materials have been studied in the framework of butanone (MEK) oxidation with a similar methodology. The light-off curves obtained for all materials are shown in Figure 3.

The values of T_{50} and T_{100} for MEK oxidation are reported in Table 3 in comparison with values corresponding to the toluene oxidation. The test conducted with SiC shows a slight conversion from 260 °C, with a MEK conversion of 20% at 400 °C. As in the case of toluene, this observation can be explained by thermal decomposition. However, this phenomenon is more important because ketone function promotes the oxidation of the molecule. For the remaining materials, firstly, the curves show greater reactivity of MEK as compared to toluene. Indeed, besides the $Pd/\alpha\text{-}Al_2O_3$ catalyst, the light-off curves are shifted to lower temperatures. This effect is particularly important for the CoAlCeO catalyst with a difference of 71 °C in the T_{50} values. Moreover, the MEK conversion at low temperature is particularly marked for the $Pd/\gamma\text{-}Al_2O_3$ and CoAlCeO catalysts. Therefore, from an activity point of view, the classification observed for the toluene oxidation on these materials is different, taking into account only the values of T_{100}. In the case of toluene, the performance sequence is: $Pd/\gamma\text{-}Al_2O_3 > Pd/\alpha\text{-}Al_2O_3 > Pd/CeO_2 > Pd/HY > CoAlCeO$. For the MEK oxidation however, the performance sequence turns as follows: $CoAlCeO > Pd/\gamma\text{-}Al_2O_3 > Pd/HY > Pd/CeO_2 > Pd/\alpha Al_2O_3$, where the CoAlCeO catalyst is now the most efficient catalyst.

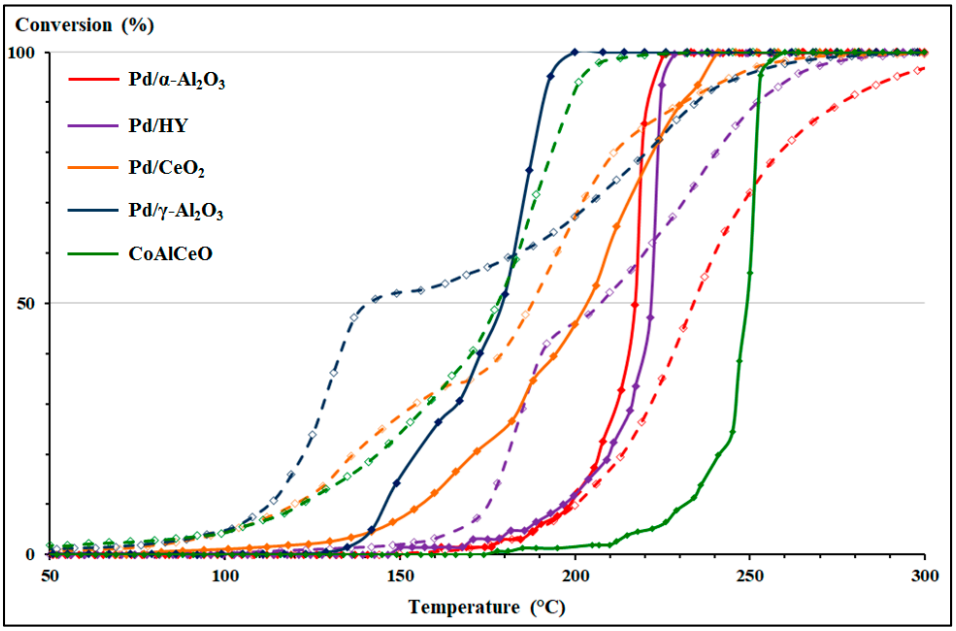

Figure 3. Comparison of light-off curves for toluene (full lines) and MEK (dashed lines) total oxidation.

Table 3. Comparison of catalyst performances for the MEK and toluene catalytic oxidation.

	MEK			Toluene		
	T_{50} (°C)	T_{100} (°C)	T_{90}–T_{10} (°C)	T_{50} (°C)	T_{100} (°C)	T_{90}–T_{10} (°C)
Pd/α-Al_2O_3	234	350	75	218	233	23
Pd/HY	207	312	77	222	242	28
Pd/CeO_2	189	347	111	197	235	75
Pd/γ-Al_2O_3	140	303	122	179	200	45
CoAlCeO	178	238	76	249	260	20

Figure 3 compares the light-off curves of toluene and MEK and clearly shows a shift of the light-off curves towards lower temperatures for MEK (dashed lines) relative to toluene (full lines). However, it is also possible to notice that these light-off curves are extended over a wider range of temperature in case of MEK oxidation. This is particularly highlighted by considering the differences between T_{90} and T_{10} values for each light-off curve (given in Table 3). In fact, this difference is on average 38 °C for toluene oxidation while it is on average 92 °C for MEK oxidation. For Pd/γ-Al_2O_3, Pd/CeO_2 and Pd/HY, the difference between the two light-off curves are substantially reduced and even reversed at high conversion: toluene indeed becomes easier to oxidize than MEK beyond a certain conversion. In addition, the light-off curves of MEK of these three catalysts exhibit an inflection point between 30% and 50% of conversion. From this point, light-off curves are stretched towards higher temperatures. In the case of Pd/α-Al_2O_3, no strong inflection point was evidenced, but the light-off curve stretches progressively with increasing temperatures. On the contrary, the light-off curve of the CoAlCeO material shows a similar behavior for both VOCs. The most important observation from this figure is the fact that the CoAlCeO catalyst achieves 100% conversion for the lowest temperature, with an important difference of approximately 65 °C with Pd/γ-Al_2O_3 and Pd/HY materials.

The profiles of the light-off curves for the MEK oxidation can be explained by the formation of byproducts. Indeed, the generation of byproducts in the case of oxygenated compounds' oxidation is relatively well known, and byproducts of MEK oxidation were identified as a result of various studies made on its partial oxidation and total oxidation [8,9,12,27,28]. Firstly, studies of McCullagh et al. [27,28], Álvarez-Galván et al. [12] and Arzamendi et al. [8] have identified three oxidation pathways that lead to several oxygenated compounds in C_2 and C_4: acetic acid, acetaldehyde, diacetyl (butane-2,3-dione) and methyl vinyl ketone. Secondly, a study realized by Machold et al. [9] has highlighted a fourth method of oxidation that leads to the formation of propanal, propanoic acid, and methanoic acid. The study of the byproducts has been applied for MEK oxidation. A microGC analysis permitted the detection of four peaks corresponding to oxidation by-products. Injection of organic standards allowed the identification of five compounds, in agreement with the literature: acetic acid (AcOOH), acetaldehyde (AcO), propionic acid (PrOOH), diacetyl (DAC), and methyl vinyl ketone (MVK). In fact, with acetic acid and acetaldehyde being co-eluted, it is not possible to differentiate and quantify them separately by micro-GC. Nevertheless, in contrast to acetic acid, acetaldehyde is carcinogenic and thus an unwanted product. Consequently, the corresponding chromatographic peak was assigned to acetaldehyde in order to consider the worst results in terms of byproduct emissions. The different byproducts have been quantified and their emission profiles have been determined as a function of MEK conversion and temperature, and are represented in Figure 4 for Pd/γ-Al_2O_3 (Figure 4a) and CoAlCeO (Figure 4b).

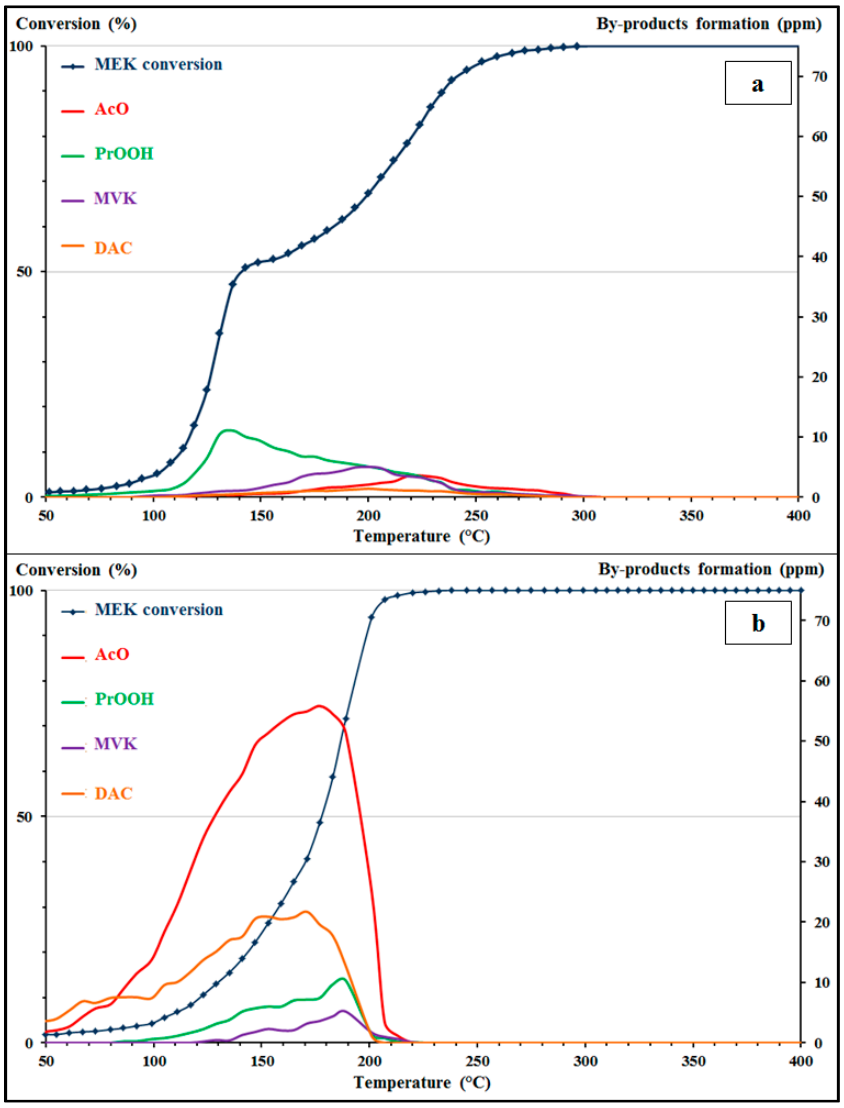

Figure 4. MEK conversion and MEK byproducts formation versus temperature for (**a**) Pd/γ-Al_2O_3 and (**b**) CoAlCeO catalysts (AcO: acetaldehyde; PrOOH: propionic acid; MVK: methyl-vinyl-ketone; DAC: diacetyl).

For the two materials Pd/γ-Al_2O_3 and CoAlCeO illustrate the two behaviors observed for the MEK oxidation. For Pd/γ-Al_2O_3, Figure 4a shows that the light-off curve is influenced by the generation of byproducts. In fact, the inflection point at 50% conversion is consistent with an emission peak of a byproduct: propionic acid. For the Pd/CeO_2 and Pd/HY materials, this inflection point is consistent with the emission peak of acetaldehyde. A hypothesis for this behavior is that these byproducts induce a partial inhibition of the MEK oxidation by blocking the catalytic sites. For CoAlCeO, the emission profiles are more important, especially for acetaldehyde (Figure 4b). However, despite this larger amount of byproducts, the material does not show any inhibitory effect on the MEK oxidation. The parameters used to characterize the benzene emission profiles were also applied on the byproducts' oxidation of MEK and are presented in Table 4.

Table 4. Parameters characterizing the emission profiles of MEK byproducts.

Pd/α-Al_2O_3	**Q_{max} (ppm)**	**T_f (°C)**	**P (°C)**	**Pd/HY**	**Q_{max} (ppm)**	**T_f (°C)**	**P (°C)**
AcO	5.4	362	+12	AcO	15.0	312	0
PrOOH	0.6	274	−76	PrOOH	11.4	312	0
MVK	2.9	350	0	MVK	1.3	312	0
DAC	2.8	322	−28	DAC	1.8	282	−30
Pd/CeO_2	**Q_{max} (ppm)**	**T_f (°C)**	**P (°C)**	**Pd/γ-Al_2O_3**	**Q_{max} (ppm)**	**T_f (°C)**	**P (°C)**
AcO	51.2	331	−16	AcO	3.6	309	+6
PrOOH	11.3	283	−64	PrOOH	11.1	303	0
MVK	3.4	300	−47	MVK	5.1	309	+6
DAC	5.6	244	−103	DAC	1.4	291	−12
CoAlCeO	**Q_{max} (ppm)**	**T_f (°C)**	**P (°C)**				
AcO	55.8	220	−18				
PrOOH	10.3	226	−12				
MVK	5.2	226	−12				
DAC	21.7	207	−31				

Table 4 reports the values of Q_{max}, T_f and P for MEK byproducts. The profiles show that acetaldehyde is the major byproduct of the MEK oxidation, except for Pd/γ-Al_2O_3. Moreover, it is possible to distinguish two emission profiles. The first can be observed for Pd/α-Al_2O_3, Pd/HY, and Pd/γ-Al_2O_3, where the maximum quantities issued for each byproduct are between 1 and 15 ppm. The second concerns Pd/CeO_2 and CoAlCeO, where these values remain on the same order of magnitude for propionic acid, methyl vinyl ketone and diacetyl, but acetaldehyde is emitted in a much larger quantity, up to 56 ppm. Finally, except for the two materials with alumina support, the byproducts seem to be fully oxidized before reaching the total conversion of MEK (T_{100}). For Pd/α-Al_2O_3 and Pd/γ-Al_2O_3, Table 4 shows a persistence of acetaldehyde. Nevertheless, this persistence is very low (6–12 °C) and has a small impact on the performance of these materials. Therefore, the sequence of performance established in relation to activities (T_{100}) remains the same after considering the byproducts: CoAlCeO > Pd/γ-Al_2O_3 > Pd/HY > Pd/CeO_2 > Pd/α-Al_2O_3.

2.4. Toluene/MEK Mixture Oxidation

The next step towards application of industrial exhaust is to study the behavior of the different catalytic materials for the total oxidation of a binary mixture (toluene/MEK 1000/1000 ppm). The results presented in this section are discussed according to two aspects: (i) the light-off curves of VOCs alone and in mixture are compared to assess mixing effects between toluene and butanone for each catalyst; (ii) the light-off curves of the binary mixture are compared in order to differentiate the performance of each catalyst. Two methods are used to calculate the VOC conversion. The first is shown in Equation (1) and denoted "$X_{Total\ Carbon}$". This allows for tracing the light-off curve in total carbon without taking into account the pressure drop and adsorption/desorption effects. Subsequently, the light-off curve is only influenced by chemical phenomena. However, this method gives a general idea and does not allow following the conversion of each VOC in the mixture. The second method is a conversion calculation taking into account the initial and outgoing quantity of VOCs. However, the light-off curve is influenced by physical phenomena (pressure drop, adsorption/desorption phenomena). The formula is given by Equation (2) and is denoted "X_{VOC}". Thus, the first method has been used to compare oxidation performances between catalysts, and the second to compare the oxidation performances between VOCs alone and in mixture.

$$X_{Total\ Carbon} = 100 \times \frac{\sum X_i \times P_{i,T} + CO_{2,\,T}}{\sum X_i \times P_{i,T} + CO_{2,\,T} + \sum X_i \times R_{i,T}} \quad (1)$$

$$X_{VOC} = 100 \times \frac{R_{i,0} - R_{i,T}}{R_{i,0}}, \quad (2)$$

where:

$R_{i,0}$ is the initial mole percentage of VOCs;
$R_{i,T}$ is the mole percentage of VOCs at the temperature T;
$P_{i,T}$ is the mole percentage of byproducts at the temperature T;
$CO_{2,T}$ is the mole percentage of carbon dioxide at the temperature T;
X_i is the number of carbon atoms in the compound i.

Concerning the mixing effects, two behaviors have been identified: inhibitory effects as well as beneficial effects. These are more or less marked as a function of the materials used and the temperature. As for the influence of MEK byproducts, these effects are more important on Pd/γ-Al_2O_3 and CoAlCeO catalysts. The light-off curves of the binary mixture for these catalysts are shown in Figure 5, and the corresponding T_{50} values are reported in Table 5.

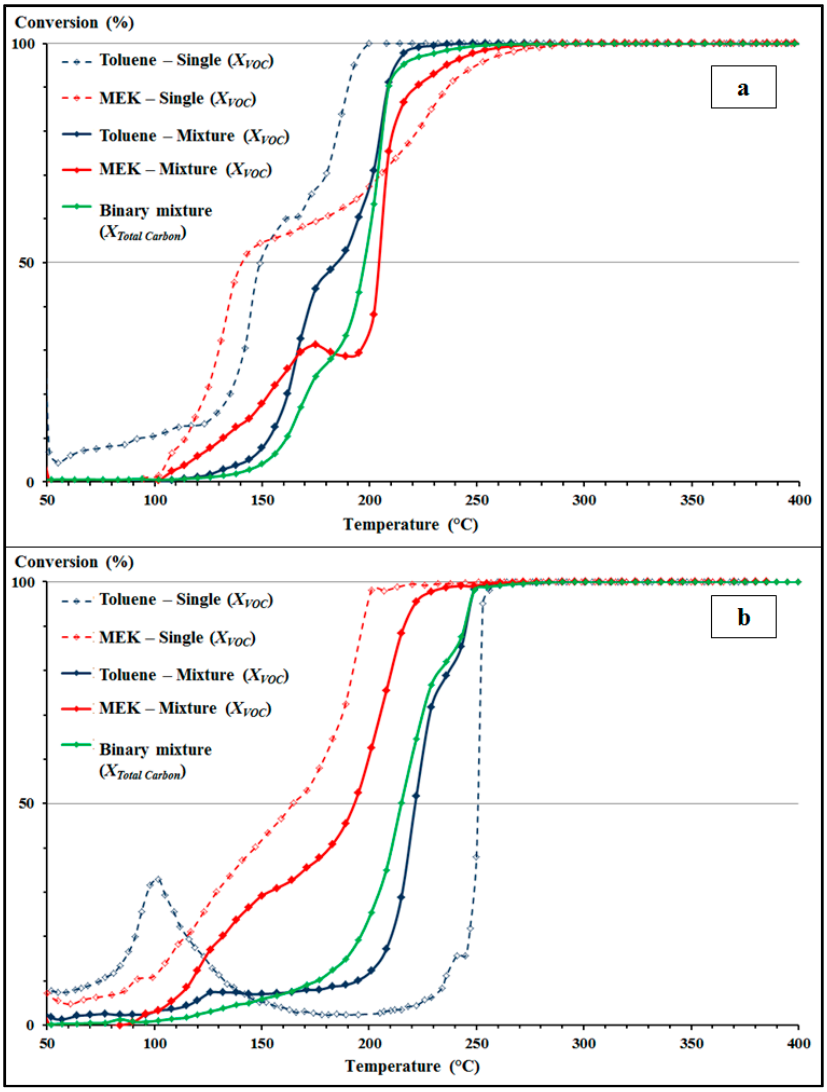

Figure 5. Light-off curves of VOCs alone and in mixture (X_{VOC} formula) and binary mixture ($X_{Total\ Carbon}$ formula) for (**a**) Pd/γ-Al_2O_3 and (**b**) CoAlCeO catalysts.

Table 5. Comparison of T_{50} for the total catalytic oxidation of binary mixture for Pd/γ-Al_2O_3 and CoAlCeO catalysts.

	Pd/γ-Al_2O_3		CoAlCeO	
	Toluene (°C)	**MEK (°C)**	**Toluene (°C)**	**MEK (°C)**
VOC alone	149	141	251	165
VOC in mixture	185	204	221	193

In the case of Pd/γ-Al_2O_3 catalyst (Figure 5a), a modification of the reactivity is revealed for both VOCs. For MEK oxidation in mixture, a shift of the light-off curve to higher temperatures is observed as compared to the light-off curve of MEK alone. Indeed, the shift between the curves begins at 100 °C on a conversion range of 0 to 70%, with a value of 63 °C at T_{50}. Beyond 70% of conversion, both light-off curves are reversed, MEK being then slightly more reactive in the presence of toluene. For toluene oxidation in mixture, a shift in the conversion curve is also observed with the light-off curve of toluene alone. Consequently, the light-off curves of VOCs in a binary mixture show inhibitory effects for both compounds. This can be explained by competitive reactions between the two molecules in the adsorption/desorption steps, causing the blocking of the active sites of the catalyst. This phenomenon has already been observed in the literature in mixtures of hydrocarbons and oxygenated compounds [7,13,29,30]. These inhibitory phenomena are also observed for Pd/HY and Pd/CeO_2.

For the CoAlCeO material (Figure 5b), the results also show a change in the reactivity of both VOCs. For MEK oxidation in mixture, a shift of the light-off curve to higher temperatures is observed. However, this effect between the two curves is more regular than with Pd/γ-Al_2O_3. A shift of 28 °C at T_{50} with the light-off curve of MEK alone is observed. In contrast, a beneficial effect is observed on the toluene oxidation in mixture. Indeed, the light-off curve of toluene in mixture is clearly shifted to lower temperatures (a difference of 30 °C at T_{50} with the toluene-alone light-off curve). This behavior can be explained by an additive effect, as has been highlighted in the studies of Beauchet et al. [31,32] for the oxidation of xylene/isopropanol mixtures. It has been shown that an intermediate compound was formed during the oxidation of this mixture, isopropyldimethylbenzene, which is obtained from the alkylation of xylene with propene, an oxidation byproduct of isopropanol. This aromatic intermediate compound possesses more alkyl chains than xylene and a ternary carbon atom, therefore its reactivity is probably higher than that of xylene. Hence, the formation of this intermediate compound lowers the temperature of xylene oxidation due to the indirect increase of its reactivity. Is has to be noted that in the case of xylene and isopropanol, the number of their respective byproducts is restricted [31,33], leading to a facilitated identification of these intermediates during the oxidation of xylene/isopropanol mixtures. In this work, both VOCs have a greater number of byproducts with almost similar structures and chemical properties [3,8,9,33]: the identification of a potential byproduct from the addition of toluene and MEK is then more difficult. Additional analyses were performed with a Omnistar Quadrupole Mass Spectrometer (QMS-200) (Pfeiffer Vacuum, Asslar, Germany), configured in "Bargraph" mode to scan all m/z fragments between 1 and 199. These analyses have failed to detect compounds other than those already known and mentioned. As a consequence, if an additional compound is formed between the toluene and MEK, its lifetime is probably too short to be detected by ex situ analysis. Enhanced catalytic activity has also been observed on the Pd/α-Al_2O_3 catalyst, but the difference was not significant.

Concerning the oxidation of the binary mixture, the light-off curves obtained are shown in Figure 6 for all materials. The values of T_{50} and T_{100} are reported in Table 6, as well as the values for the oxidation of toluene for comparison.

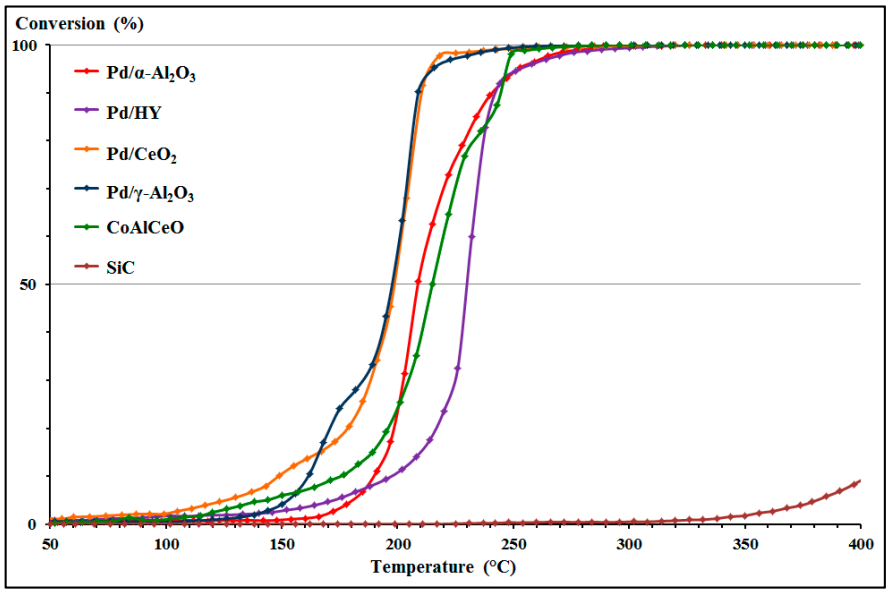

Figure 6. Light-off curves of binary mixture total oxidation.

Table 6. T_{50} and T_{100} of catalysts for binary mixture and toluene catalytic oxidation.

Catalyst	Binary Mixture		Toluene	
	T_{50} (°C)	T_{100} (°C)	T_{50} (°C)	T_{100} (°C)
Pd/α-Al_2O_3	209	326	218	233
Pd/HY	230	330	222	242
Pd/CeO_2	199	314	197	235
Pd/γ-Al_2O_3	198	290	179	200
CoAlCeO	215	290	249	260

The test conducted with SiC shows a slight conversion of the binary mixture from 225 °C, with a maximum of 9.9% at 400 °C. This partial conversion is derived from the thermal decomposition of VOCs, primarily of MEK, as has been observed for blank experiments performed with pure VOCs. In addition, partial conversion of the mixture begins at 225 °C instead of 260 °C and 360 °C, respectively, for MEK and toluene used on their own. However, partial conversion of the mixture reached a maximum of 9.9% (198 ppm) at 400 °C instead of 20.6% (206 ppm) and 5.7% (57 ppm), respectively, for MEK and toluene. Thus, the binary mixture seems to be reactive at lower temperatures, but with more limited conversion rates at high temperatures. As a first proof, the tests show light-off curves much less stretched than in the case of MEK oxidation. In addition, mixing effects observed for palladium-based catalysts do not significantly modify their performance. Indeed, given the T_{50} values, they remain close to those observed during toluene oxidation, with only a small temperature difference. Nevertheless, the mixing effects observed for the CoAlCeO mixed oxide have a strong impact on its activity: this is the least active catalyst for oxidation of toluene alone, without considering the byproduct oxidation. For the binary mixture, the presence of the MEK significantly lowers the value of T_{50} and this material exhibits performance fully comparable to palladium-based catalysts. As a second proof, beyond 95% of conversion, the light-off curves significantly stretch, which is correlated with a strong persistence of the residual traces of VOCs in the flow, especially for MEK. Therefore, the T_{100} values for the binary mixture oxidation are more important for all materials with respect to the oxidation of toluene alone, with an average shift of 88 °C. This phenomenon was expected since the total VOC concentration is higher in the binary mixture (2000 ppm instead of 1000 ppm). An important point is that only CoAlCeO mixed oxide presents a reduced impact of this phenomenon with only 30 °C difference on its T_{100} value. As a conclusion, this oxide corresponds to one of the best catalyst for the total abatement of

the binary mixture. According to the T_{50} and T_{100}, the performance sequence observed for the binary mixture oxidation is the following: CoAlCeO = Pd/γ-Al_2O_3 > Pd/CeO_2 > Pd/α-Al_2O_3 > Pd/HY.

Regarding the effect of byproducts on the behavior of the mixture, their profiles were followed according to the conversion and temperature. The results show the emission of all byproducts already detected during the study of toluene and MEK oxidation: benzene, acetaldehyde (AcO), propionic acid (PrOOH), methyl vinyl ketone (MVK), and diacetyl (DAC). Additionally, the emission profiles present significant changes due to the mixing effects. Indeed, the persistence, *P*, and the maximum quantity emitted observed Q_{max}, are significantly changed. Figure 7 shows the emission profiles of the byproducts from the binary mixture oxidation on Pd/CeO_2.

This catalyst exhibits the most remarkable and representative impacts of mixing effects on byproducts' emission profiles. Table 7 reports values of Q_{max}, T_f, and *P* for the binary mixture, as well as the values for oxidation of toluene and MEK alone for comparison.

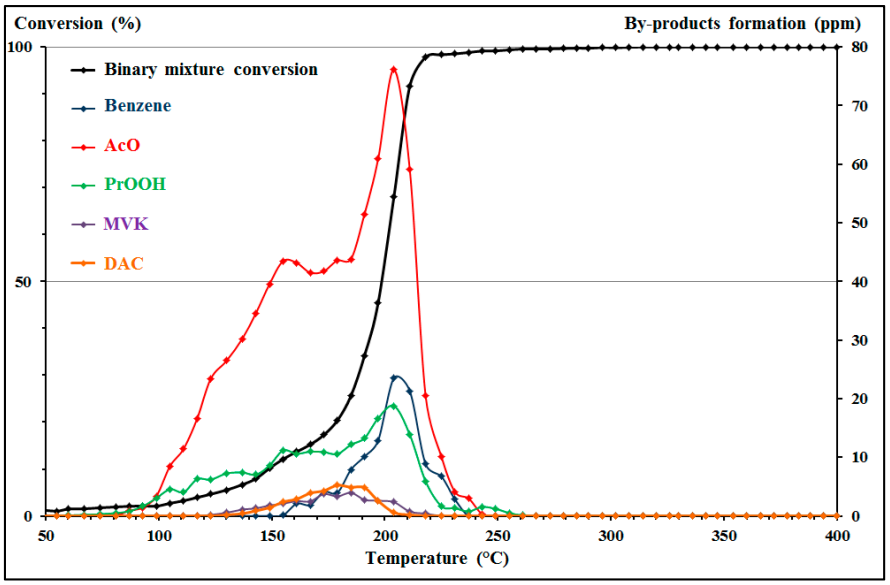

Figure 7. Binary mixture conversion and byproduct formation versus temperature for Pd/CeO_2 catalyst.

Table 7. Parameters characterizing the emission profiles on Pd/CeO_2 of byproducts for VOCs alone and in binary mixture.

Toluene	Q_{max} **(ppm)**	T_f **(°C)**	*P* **(°C)**
Benzene	7.0	298	63
MEK	Q_{max} **(ppm)**	T_f **(°C)**	*P* **(°C)**
AcO	51.2	331	−16
PrOOH	11.3	283	−64
MVK	3.4	300	−47
DAC	5.6	244	−103
Binary Mixture	Q_{max} **(ppm)**	T_f **(°C)**	*P* **(°C)**
Benzene	23.6	237	−77
AcO	76.1	249	−65
PrOOH	18.8	267	−47
MVK	4.0	225	−89
DAC	5.2	218	−96

The mixing effects mainly impact on the values of *P* and Q_{max}. Regarding the persistence, *P*, the values decrease significantly for several compounds. This observation indicates that byproducts

are eliminated at a lower temperature. This is particularly true for benzene whose P value is +63 °C for toluene oxidation instead of −77 °C for binary mixture oxidation. As mentioned before, this effect is especially beneficial due to the toxicity of this compound. Propionic acid is the only byproduct here whose persistence increases significantly, although the value is still negative. Concerning Q_{max} values, the emission peaks of benzene, acetaldehyde, and propionic acid are observed. This proves that even though these compounds are more easily oxidized, they are also emitted in larger amounts. In a different way to these three compounds, the values of Q_{max} observed for the methyl vinyl ketone and diacetyl show very slight variations, and these two compounds are present as minority byproducts. This observation is also carried out for all materials studied on the binary mixture. To simplify the comparison between materials, only benzene, acetaldehyde, and propionic acid will be considered thereafter. Table 8 reports the Q_{max}, T_f, and P values of these three compounds for the five materials. This table highlights the significant reduction in the persistence of benzene.

Table 8. Parameters characterizing the emission profiles of binary mixture byproducts.

Pd/α-Al_2O_3	**Q_{max} (ppm)**	**T_f (°C)**	**P (°C)**	**Pd/HY**	**Q_{max} (ppm)**	**T_f (°C)**	**P (°C)**
Benzene	11.5	361	+35	Benzene	9.9	282	−48
AcO	7.6	320	−6	AcO	8.5	336	+6
PrOOH	1.3	314	−12	PrOOH	4.8	306	−24
Pd/CeO_2	**Q_{max} (ppm)**	**T_f (°C)**	**P (°C)**	**Pd/γ-Al_2O_3**	**Q_{max} (ppm)**	**T_f (°C)**	**P (°C)**
Benzene	23.6	237	−77	Benzene	26.5	296	+6
AcO	76.1	249	−65	AcO	3.8	266	−24
PrOOH	18.8	267	−47	PrOOH	11.6	260	−30
CoAlCeO	**Q_{max} (ppm)**	**T_f (°C)**	**P (°C)**				
Benzene	4.0	272	−18				
AcO	73.7	255	−35				
PrOOH	15.5	236	−54				

Indeed, except for the two materials with an alumina support, the persistence of benzene is negative, but has nonetheless been greatly reduced since these values have increased from +6 °C to +35 °C and +44 °C instead of +67 °C, respectively, for the oxidation of toluene alone. Regarding acetaldehyde and propionic acid, the tests show a relative increase in Q_{max} values as compared to those for MEK alone. Similarly, the persistence of acetaldehyde emissions is greatly reduced for all materials except Pd/HY. For the persistence of propionic acid, the behavior is more variable, though: a slight increase is observed for Pd/α-Al_2O_3 and Pd/CeO_2, while a decrease is observed for Pd/HY, Pd/γ-Al_2O_3 and CoAlCeO. Considering these facts, the study of the total oxidation of the binary mixture highlights the two most efficient catalytic materials: the commercial formulation Pd/γ-Al_2O_3 and the mixed oxide CoAlCeO. Indeed, these materials show the same performance in terms of activity with a T_{100} to 290 °C for both materials. Considering the byproducts, the mixed oxide has a slight advantage over Pd/γ-Al_2O_3 since the byproducts are completely eliminated at 290 °C. Considering this fact, the performance sequence is as follows: CoAlCeO > Pd/γ-Al_2O_3 > Pd/CeO_2 > Pd/HY > Pd/αAl_2O_3.

2.5. Oxidation of a Simulated Industrial Exhaust

The literature on VOCs' oxidation systematically studied models exhausts where VOCs' concentration and flow rate are perfectly controlled, while only a few articles focus on the study of VOCs mixtures [7,13–18,31,32]. As in this study, these articles highlight different inhibitory or beneficial effects derived from interactions between compounds. However, a binary or ternary mixture studied at the laboratory level remains far from the reality of an industrial effluent, which can be made up of many more compounds (10 to 50 compounds) with variable compositions and concentrations over time. To get closer to industrial applications, we further studied a more complex mixture of VOCs

that was established based on the composition of an industrial effluent and will therefore be referred to as a simulated industrial exhaust. In the industry, part of the manufacturing process is to apply lacquers and paints to metal surfaces, the consequence being that industry emits significant amounts of gaseous effluents with a high concentration of VOCs and a high flow rate. These effluents contain mostly aromatic compounds, mainly toluene, and oxygenated compounds, mainly MEK, as well as traces of paraffins (C_9–C_{11}). The liquid mixture used here to simulate the industrial effluent of VOCs was constituted by selecting six aromatic compounds (toluene, o-xylene, ethylbenzene, propylbenzene, 4-ethylbenzene, and 1,4diethylbenzene), three oxygenates (butanone, butanol, butoxyethanol), and a paraffin (decane). The concentration of each substance is fixed to a concentration of 10 vol% in the liquid phase. This mixture was studied on the same experimental setup as in previous studies, the mixture being placed in a saturator. The temperature of the saturator was set so as to fix a value of 7000 ppm carbon equivalent (ppm eq. C) in a 100 mL·min^{-1} air flow, with a total hydrocarbons analyzer COSMA Graphite 655 (Environnement SA, Poissy, France). The gas phase composition determined by microGC is given in Figure 8.

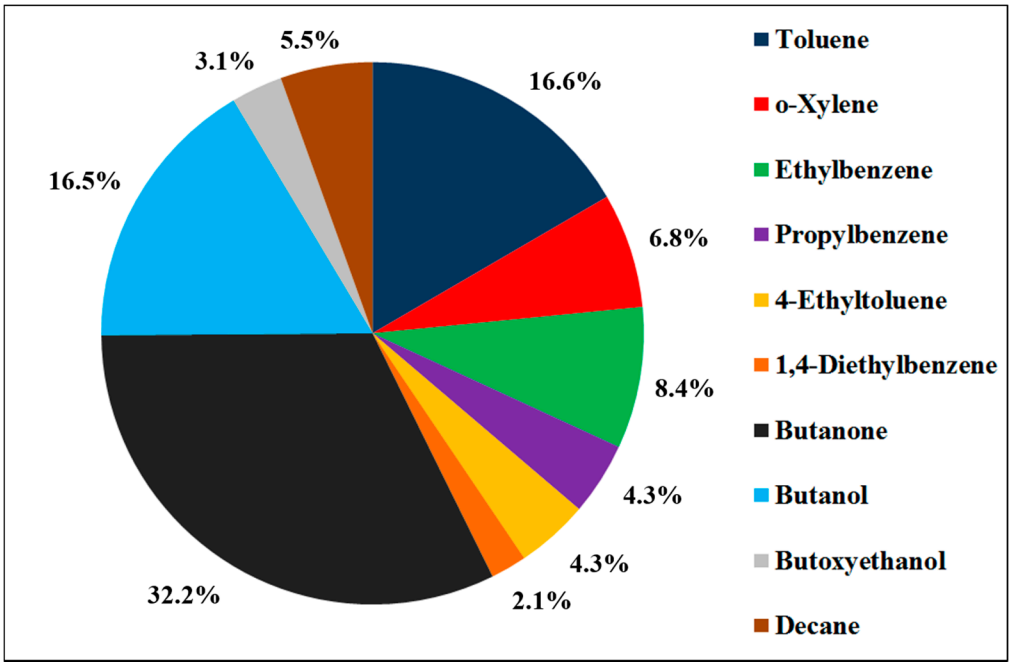

Figure 8. Composition of the complex mixture determined by μGC.

In order to place themselves under real measurement conditions, the abatement rate of VOCs mixture is measured with a total hydrocarbons analyzer (COSMA Graphite 655), equivalent to a flame ionization detector (FID). Indeed, VOC measurements on industrial effluents are performed with this type of device, and this measuring method conforms to a French regulatory norm (NF X 43-301). Furthermore, although the microGC is a suitable tool for measuring VOCs' oxidation, this technique reaches its limits with regards to the detection and separation of the various molecules that can be emitted or generated during the process. The abatement curves obtained by the total hydrocarbons analyser (measurements given in equivalent carbon (eq. C)) are comparable to light-off curves determined by microGC. Nevertheless, microGC was used as a complementary analytic device, as well as trapping on cartridge Tenax TA (Supelco, Bellefonte, PA, USA) and Mass Spectrometer QMS-200 (Pfeiffer Vacuum, Asslar, Germany), for speciation analysis. Finally, this study has been conducted with the two catalysts presenting the best performances: Pd/γ-Al_2O_3 and CoAlCeO. These two materials appear to be most effective for the abatement of the VOCs studied and their resulting byproducts. This choice is relevant for two main reasons: Firstly, Pd/γ-Al_2O_3 is an efficient commercial

catalyst that is sold for such industrial applications and is thus suitable as a benchmark. Secondly, CoAlCeO is an alternative formulation exhibiting an efficiency similar to or even better than the commercial material. In addition, this material is not made of noble metals and its cost is considerably lower as compared to the commercial formulation. The abatement curves obtained, expressed in ppm carbon equivalent (ppm eq. C) versus temperature, are given in Figure 9. The T_{50} values are reported in Table 9, where the values for the oxidation of toluene and binary mixture are also reported for comparison.

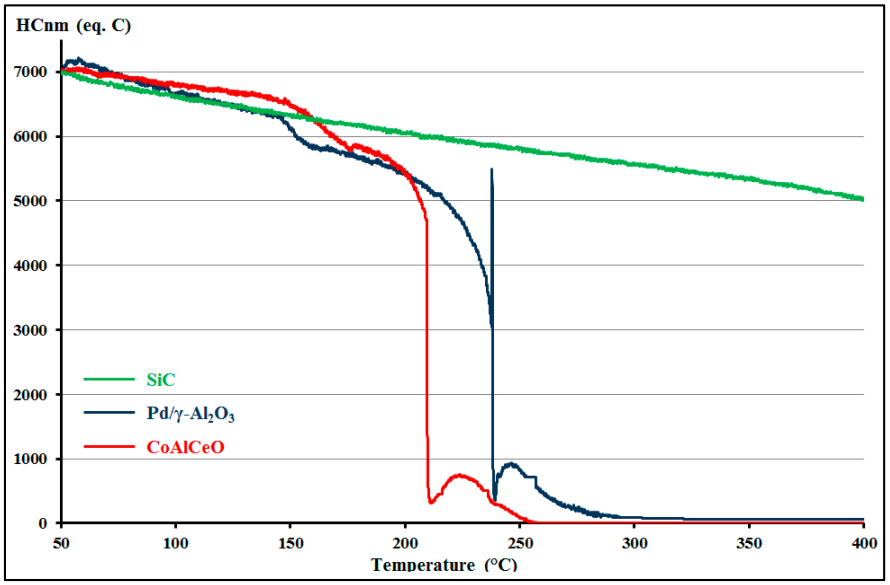

Figure 9. Abatement curves of the complex mixture on Pd/γ-Al_2O_3 and CoAlCeO catalysts.

Table 9. T_{50} of Pd/γ-Al_2O_3 and CoAlCeO catalysts for toluene, binary mixture, and complex mixture total oxidation.

	Toluene (°C)	Binary Mixture (°C)	Complex Mixture (°C)
Pd/γ-Al_2O_3	179	198	237
CoAlCeO	249	215	210
Δ	+70	+17	−27

The test performed on the SiC shows a partial conversion of the complex mixture, with a maximum of 28.1% at 400 °C. This relatively high conversion is due to the thermal decomposition of oxygenates (MEK, butan-1-ol and butoxyethanol). This was confirmed by microGC analyses that highlight some byproducts: acetaldehyde, propionic acid, methyl vinyl ketone and diacetyl, which are derived from the MEK oxidation and butanal and 1-butene, which are derived from the butan-1-ol conversion (partial oxidation and dehydration, respectively). In addition, analyses do not show the presence of CO_2, which confirms partial oxidation only. The results show an abatement of 99.2% and 100% of the complex mixture for Pd/γ-Al_2O_3 and CoAlCeO, respectively. In addition, the abatement curves do not exhibit a sigmoidal profile characteristic of the light-off curves. The conversion observed between 0% and 20% is due to the decomposition of oxygenates, mainly butan-1-ol and butoxyethanol, leading to the corresponding aldehydes and acids (butanal, acetaldehyde, and acetic acid). The degradation of aromatic compounds is only starting at 155 and 175 °C for CoAlCeO and Pd/γ-Al_2O_3, respectively. Then, the mixture conversion abruptly increases from 30 to 95% for CoAlCeO and from 55 to 95% for Pd/γ-Al_2O_3 in just seconds. This is accompanied by an overpressure/depression phenomenon, confirmed by mass spectrometry, and an immediate increase of 30 °C of the reactor temperature. This is characteristic of a deflagration effect, which explains the appearance of abatement curves.

This phenomenon is slower on Pd/γ-Al_2O_3, and also more visible. Moreover, a peak of methane emission is measured by the total hydrocarbons analyzer. Finally, the system returns to a steady state, with a slight loss of conversion, before the degradation of the residual organic fraction is performed until the maximum conversion is reached.

Concerning the performance, Pd/γ-Al_2O_3 presents a T_{50} values around 40 °C greater than in the binary mixture case, highlighting a more significant inhibition effect. In addition, conversion of the complex mixture stabilizes at 99.2% at 325 °C. Additional analyses at 325 (T_{99}), 350, and 400 °C show that the remaining organic fraction is predominantly composed of decane and benzene, as well as a small proportion of MEK. For CoAlCeO, the T_{50} value is lowered once more in comparison with the binary mixture and toluene oxidation, but to a lower extent with only 5 °C on T_{50} between the complex and binary mixture. Moreover, conversion of the complex mixture reaches 100% from 357 °C. Additional analysis at 325 (T_{99}) and 350 °C show that the residual organic fraction is composed of MEK and toluene, with MEK being predominant. The same analysis conducted at 400 °C confirms a total abatement of the mixture. Therefore, the CoAlCeO mixed oxide is highlighted as a promising alternative material to the commercial Pd/γ-Al_2O_3 catalyst, with the latter currently being used for industrial units' VOCs treatment. Indeed, CoAlCeO shows the best performance for the complex mixture oxidation considering the rate and temperature of VOCs abatement. In addition, no toxic compounds seem to be emitted at high conversion by this catalyst.

3. Materials and Methods

3.1. Synthesis of the Palladium Impregnated Materials

3.1.1. Preparation of Supports

Ceria support was prepared by a precipitation method. A solution of $Ce(NO_3)_3 \cdot 6H_2O$ (Fisher Scientific, Hampton, NH, USA) was added drop by drop to a NaOH (Fisher Scientific, Hampton, NH, USA) solution with a molar ratio Ce^{3+}/OH^- of 1/5. The addition was made under magnetic stirring over 3 h. The suspension was left under stirring for 2 h at ambient temperature. Then, the suspension was filtered and washed six times with 200 mL of hot deionized water (~60 °C). The solid was dried for 24 h at 100 °C and calcined for 4 h at 500 °C (1 °C·min^{-1}) under air flow (2 L·h^{-1}).

HY Faujasite zeolite was prepared by ionic exchange. A commercial NaY Faujasite zeolite (Si/Al: 2.7; Sigma-Aldrich, St. Louis, MO, USA) was slurried in a solution of ammonium nitrate 2.0 mol·L^{-1} with a molar ration NH_4^+/Na^+ of 20. The suspension was maintained for 18 h at 80 °C under magnetic agitation. Then, the suspension was filtered and washed with hot deionized water (~60 °C) to a neutral pH. These operations were repeated three times. Then, the solid was dried overnight at 100 °C and calcined for 4 h at 400 °C (1 °C·min^{-1}) under air flow (2 L·h^{-1}).

For the α-Al_2O_3, a commercial powder was chosen (ACROS ORGANICS, 99.0%).

3.1.2. Palladium Impregnation

Palladium (Fisher Scientific, Hampton, NH, USA) was deposed on support (α-Al_2O_3, CeO_2, and HY Faujasite) by aqueous impregnation method (0.5 wt % Pd). Solid was suspended in an appropriate volume of palladium nitrate solution (0.25 g·L^{-1}). The suspension was maintained for 18 h at 60 °C. Then, water was removed by a rotary evaporator. The solid was dried overnight at 100 °C and then calcined for 4 h at 400 °C (1 °C·min^{-1}) under air flow (2 L·h^{-1}).

A commercial Pd/γ-Al_2O_3 catalyst (ACROS ORGANICS, 0.5 wt %) was chosen to complete the study.

3.2. Synthesis of the Mixed Oxide

The CoAlCe mixed oxide was synthesized in the hydrotalcite way. An aqueous solution of 200 mL was prepared with $Co(NO_3)_2 \cdot 6H_2O$, $Al(NO_3)_3 \cdot 9H_2O$ and $Ce(NO_3)_3 \cdot 6H_2O$ (Fisher Scientific, Hampton,

NH, USA), with a molar ratio of $Co^{2+}/Al^{3+}/Ce^{3+}$ of 6/1.2/0.8 ($Co_6Al_{1.2}Ce_{0.8}O_x$). This solution was added drop by drop to 30 mL of a Na_2CO_3 (Fisher Scientific, Hampton, NH, USA) solution (1 mol·L^{-1}). The pH of the additive solution was maintained at a value of 10.5 with a NaOH solution (2 mol·L^{-1}). After addition, the suspension was stirred for 18 h at room temperature. Then, the latter was filtered and washed with hot deionized water (~60 °C). The solid obtained was dried in an oven for 24 h at 60 °C and ground before being calcined for 4 h at 500 °C (1 °C·min^{-1}) under air flow (2 L·h^{-1}) and given the code name CoAlCeO.

3.3. Characterization of the Catalysts

Crystalline structures were determined at room temperature from X-ray Diffraction (XRD) recorded on a D8 Advance diffractometer (Bruker AXS, Billerica, MA, USA) equipped with a copper anode (λ = 1.5406 Å) and a LynxEye Detector. The scattering intensities were measured over an angular range of $10° \leq 2\theta \leq 80°$ for all samples with a step size of $\Delta(2\theta) = 0.02°$ and a count time of 4 s per step. The diffraction patterns were indexed by comparison with the "Joint Committee on Powder Diffraction Standards" (JCPDS) files.

Specific surface areas (SBET) were determined by the Brunauer–Emmet–Teller method on N_2 isotherms measured with a ThermoElectron Qsurf M1 series Surface Area Analyzer apparatus (Waltham, MA, USA). The sample was degassed before measurement at 130 °C under helium flow. Adsorption was made with a 30% N_2−70% He mixture at −196 °C. Desorption of gaseous N_2 was quantified with a thermal conductivity detector.

For the elemental analysis, 50.0 mg of powder was dissolved in 5 mL of aqua regia (HNO_3/HCl 1:2) (Fisher Scientific, Hampton, NH, USA) under microwave for 30 min (CEM, Model MARSXpress, Matthews, CA, USA). Then, the solution was extended to 50.0 mL with ultrapure water and filtered with a 0.45-µm cellulosic micro-filter. Analysis was performed with an ICP-OES (Thermo, model ICAP 6300 Duo, Waltham, MA, USA).

Hydrogen chemisorption was realized with 0.5 g of catalysts mixed with 0.5 g of silicon carbide, in order to have a homogeneous catalytic bed and avoid hot spots. The mixture was reduced for 2 h at 200 °C (3 °C·min^{-1}) under dihydrogen flow (30 mL·min^{-1}). Then, the system was cooled down to 80 °C under an argon flow (30 mL·min^{-1}). A step of 30 min under argon flow (30 mL·min^{-1}) was realized, followed by a step of 30 min under 10% H_2/Ar flow (30 mL·min^{-1}) and a last step of 30 min under argon flow (30 mL·min^{-1}). Finally, desorption was performed under a flow of argon (30 mL·min^{-1}) from 80 to 475 °C (10 °C·min^{-1}), followed by a step of 10 min. The detector used was a mass spectrometer Balzers QMG 422 MS (Pfeiffer Vacuum, Asslar, Germany).

3.4. Catalytic Tests

Total oxidation of VOCs was studied in a fixed bed reactor loaded with 100 mg of catalyst. VOC/Air mixtures were generated with a saturator in order to obtain 1000 ppm of VOC in a flow of 100 mL·min^{-1}. A toluene/MEK binary mixture was generated in order to obtain 1000 ppm of each VOC in a flow of 100 mL·min^{-1}. Tests were made between 50 and 400 °C with a temperature ramp of 1.5 °C·min^{-1}. Catalysts were pre-treated for 2 h at 200 °C (1 °C·min^{-1}) under air flow (2 L·h^{-1}) and then, for impregnated catalysts, were reduced for 2 h at 200 °C (1 °C·min^{-1}) under dihydrogen (5.0) flow (2 L·h^{-1}). Organic compounds were analyzed by gas chromatography with a CP-4900 microGC (Agilent Technologies Inc., Santa Clara, CA, USA). A test was systematically conducted under the same conditions with silicon carbide SiC to achieve a blank experiment.

Catalytic performances were compared considering the T_{50} and T_{100}, which correspond to the temperature at which 50% and 100% of VOC, respectively, were converted. VOC conversion was calculated considering products and byproducts and as a function of the number of carbons for each compound:

$$X_T = 100 \times \frac{\sum X_i \times P_{i,T} + CO_{2,T}}{\sum X_i \times P_{i,T} + CO_{2,T} + \sum X_i \times R_{i,T}} \quad (3)$$

where:

$P_{i,T}$ is the mole percentage of VOCs at the temperature T;
$P_{i,T}$ is the mole percentage of byproducts at the temperature T;
$CO_{2,T}$ is the mole percentage of carbon dioxide at the temperature T;
X_i is the carbon number of corresponding compounds.

Catalytic activity was calculated at a VOC conversion of 20% and considering a plug-flow reactor:

$$A = \frac{Q}{V_M} \cdot \frac{273.15}{T_{20}} \cdot \frac{R_{i,o}}{10^6} \cdot \frac{X}{m} \cdot \frac{1}{S_{BET}} \quad (4)$$

where:

Q is the volume flow ($L \cdot h^{-1}$);
V_M is the molar volume ($L \cdot mol^{-1}$);
T_{20} is the catalyst temperature for 20% VOC conversion (K);
$R_{i,o}$ is the VOC initial concentration (ppm);
X is the VOC conversion (%);
m is the catalyst mass (g);
S_{BET} is the specific surface area of the catalyst ($m^2 \cdot g^{-1}$).

4. Conclusions

Catalytic oxidation appears to be an efficient VOC treatment process that is more cost-effective and environmentally friendly than thermal oxidation. Nevertheless, the cost of the catalytic materials remains an obstacle to the wider use of this process at an industrial level. Indeed, the most efficient catalysts are generally constituted of precious metals (Pt, Pd, Pt-Pd). The aim of this work was to propose an alternative material to the materials commonly used for this application. To bring this to fruition, a CoAlCeO mixed oxide was developed in the laboratory, and was compared to palladium-based catalysts ($Pd/\alpha\text{-}Al_2O_3$, Pd/CeO_2, Pd/HY and a commercial $Pd/\gamma\text{-}Al_2O_3$) for the total oxidation of industrial VOCs: toluene and butanone (MEK). These VOCs were selected as model molecules in agreement with their use in industry as a solvent in paints, inks and varnishes for application on metal surfaces. The study was conducted for these five materials on the total oxidation of toluene, MEK, and a toluene/MEK binary mixture. The study was also carried out taking into account the formation of byproducts in the catalytic performance. Tests have shown various results for the three sets of experiments presented in this study. Different performances, as well as inhibition or beneficial effects, were identified. Nevertheless, all the results highlight the two most effective materials for the oxidation of VOCs, but also for oxidation of their byproducts: $Pd/\gamma\text{-}Al_2O_3$ and CoAlCeO. The results obtained with the commercial formulation $Pd/\gamma\text{-}Al_2O_3$ were expected since it is one of the formulations typically used for this industrial process; its effectiveness has been already demonstrated. Therefore, our results on CoAlCeO mixed oxide highlight their efficiency and put forward this material as a relevant alternative to conventional Pd-based catalysts. The estimated cost of the CoAlCeO catalyst used in this study, based on the price of the metallic precursors and the chemical species used, is around 30% lower than the $Pd/\gamma\text{-}Al_2O_3$ catalyst. Thus, this oxide opens up the development of new, efficient and less expensive catalysts for this treatment process.

Acknowledgments: The authors wish to acknowledge the "Agency of Environment and Energy Management" (ADEME) as well as the Nord-Pas-de-Calais region for the funding of the work (project number 1281C0095). The authors also acknowledge the "Centre Commun de Mesures" of ULCO. Cédric Barroo thanks the Fonds de la Recherche Scientifique (F.R.S.-FNRS) for financial support.

Author Contributions: Julien Brunet and Eric Genty performed the material preparation and the experiments. Cédric Barroo, Fabrice Cazier, Christophe Poupin, Stéphane Siffert, Diane Thomas, Guy De Weireld, and Thierry Visart de Bocarmé revised and modified the paper. All authors contributed equally to the data

interpretation and discussion. Julien Brunet, Eric Genty, Cédric Barroo, and Renaud Cousin wrote the final manuscript. Renaud Cousin conceived and managed the project.

Conflicts of Interest: The authors declare no conflict of interest.

References

1. Hu, C. Catalytic combustion kinetics of acetone and toluene over $Cu_{0.13}Ce_{0.87}O_y$ catalyst. *Chem. Eng. J.* **2011**, *168*, 1185–1192. [CrossRef]
2. Liotta, L.F.; Ousmane, M.; Di Carlo, G.; Pantaleo, G.; Deganello, G.; Boreave, A.; Giroir-Fendler, A. Catalytic removal of toluene over Co_3O_4–CeO_2 mixed oxide catalysts: Comparison with Pt/Al_2O_3. *Catal. Lett.* **2008**, *127*, 270–276. [CrossRef]
3. Brunet, J.; Genty, E.; Landkocz, Y.; Al Zallouha, M.; Billet, S.; Courcot, D.; Siffert, S.; Thomas, D.; De Weireld, G.; Cousin, R. Identification of by-products issued from the catalytic oxidation of toluene by chemical and biological methods. *Comptes Rendus Chim.* **2015**, *18*, 1084–1093. [CrossRef]
4. Genty, E.; Cousin, R.; Capelle, S.; Gennequin, C.; Siffert, S. Catalytic oxidation of toluene and CO over nanocatalysts derived from hydrotalcite-like compounds ($X_6^{2+}Al_2^{3+}$): Effect of the bivalent cation. *Eur. J. Inorg. Chem.* **2012**, *2012*, 2802–2811. [CrossRef]
5. Santos, V.P.; Pereira, M.F.R.; Órfão, J.J.M.; Figueiredo, J.L. Mixture effects during the oxidation of toluene, ethyl acetate and ethanol over a cryptomelane catalyst. *J. Hazard. Mater.* **2011**, *185*, 1236–1240. [CrossRef] [PubMed]
6. Wu, H.; Wang, L.; Zhang, J.; Shen, Z.; Zhao, J. Catalytic oxidation of benzene, toluene and *p*-xylene over colloidal gold supported on zinc oxide catalyst. *Catal. Commun.* **2011**, *12*, 859–865. [CrossRef]
7. Burgos, N.; Paulis, M.; Mirari Antxustegi, M.; Montes, M. Deep oxidation of VOC mixtures with platinum supported on Al_2O_3/Al monoliths. *Appl. Catal. B Environ.* **2002**, *38*, 251–258. [CrossRef]
8. Arzamendi, G.; de la Peña O'Shea, V.A.; Álvarez-Galván, M.C.; Fierro, J.L.G.; Arias, P.L.; Gandía, L.M. Kinetics and selectivity of methyl-ethyl-ketone combustion in air over alumina-supported PdO_x-MnO_x catalysts. *J. Catal.* **2009**, *261*, 50–59. [CrossRef]
9. Machold, T.; Suprun, W.Y.; Papp, H. Characterization of VO_x-TiO_2 catalysts and their activity in the partial oxidation of methyl ethyl ketone. *J. Mol. Catal. A Chem.* **2008**, *280*, 122–130. [CrossRef]
10. Gandía, L.M.; Gil, A.; Korili, S.A. Effects of various alkali-acid additives on the activity of a manganese oxide in the catalytic combustion of ketones. *Appl. Catal. B Environ.* **2001**, *33*, 1–8. [CrossRef]
11. Paulis, M.; Gandia, L.M.; Gil, A.; Sambeth, J.; Odriozola, J.A.; Montes, M. Influence of the surface adsorption–desorption processes on the ignition curves of volatile organic compounds (VOCs) complete oxidation over supported catalysts. *Appl. Catal. B Environ.* **2000**, *26*, 37–46. [CrossRef]
12. Álvarez-Galván, M.C.; de la Peña O'Shea, V.A.; Arzamendi, G.; Pawelec, B.; Gandía, L.M.; Fierro, J.L.G. Methyl ethyl ketone combustion over La-transition metal (Cr, Co, Ni, Mn) perovskites. *Appl. Catal. B Environ.* **2009**, *92*, 445–453. [CrossRef]
13. Tsou, J.; Magnoux, P.; Guisnet, M.; Orfao, J.J.M.; Figueiredo, J.L. Catalytic oxidation of volatile organic compounds: Oxidation of methyl-isobutyl-ketone over Pt/zeolite catalysts. *Appl. Catal. B Environ.* **2005**, *57*, 117–123. [CrossRef]
14. Li, W.B.; Wang, J.X.; Gong, H. Catalytic combustion of VOCs on non-noble metal catalysts. *Catal. Today* **2010**, *148*, 81–87. [CrossRef]
15. Papaefthimiou, P.; Ioannides, T.; Verykios, X. Combustion of non-halogenated volatile organic compounds over group VIII metal catalysts. *Appl. Catal. B Environ.* **1997**, *13*, 175–184. [CrossRef]
16. Liotta, L.F. Catalytic oxidation of volatile organic compounds on supported noble metals. *Appl. Catal. B Environ.* **2010**, *100*, 403–412. [CrossRef]
17. Ordóñez, S.; Bello, L.; Sastre, H.; Rosal, R.; Fernando, V.D. Kinetics of the deep oxidation of benzene, toluene, *n*-hexane and their binary mixtures over a platinum on γ-alumina catalyst. *Appl. Catal. B Environ.* **2002**, *38*, 139–149. [CrossRef]
18. Barressi, A.A.; Baldi, G. Deep catalytic oxidation of aromatic hydrocarbon mixtures: Reciprocal inhibition effects and kinetics. *Ind. Eng. Chem. Res.* **1994**, *33*, 2964–2974. [CrossRef]
19. Rusu, A.O.; Dumitriu, E. Destruction of volatile organic compounds by catalytic oxidation. *Environ. Eng. Manag. J.* **2003**, *2*, 273–302. [CrossRef]

20. Papaefthimiou, P.; Ioannides, T.; Verykios, X.E. Catalytic incineration of volatile organic compounds present in industrial waste streams. *Appl. Therm. Eng.* **1998**, *18*, 1005–1012. [CrossRef]
21. Centi, G. Supported palladium catalysts in environmental catalytic technologies for gaseous emissions. *J. Mol. Catal. A Chem.* **2001**, *173*, 287–312. [CrossRef]
22. Forzatti, P.; Lietti, L. Catalyst deactivation. *Catal. Today* **1999**, *52*, 165–181. [CrossRef]
23. Genty, E.; Brunet, J.; Pequeux, R.; Capelle, S.; Siffert, S.; Cousin, R. Effect of Ce substituted hydrotalcite-derived mixed oxides on total catalytic oxidation of air pollutant. *Mater. Today Proc.* **2016**, *3*, 277–281. [CrossRef]
24. Hibino, T.; Tsunashima, A. Formation of spinel from a hydrotalcite-like compound at low temperature: Reaction between edges of crystallites. *Clays Clay Miner.* **1997**, *45*, 842–853. [CrossRef]
25. Bera, P.; Rajamathi, M.; Hegde, M.S.; Kamath, P.V. Thermal behaviour of hydroxides, hydroxysalts and hydrotalcites. *Bull. Mater. Sci.* **2000**, *23*, 141–145. [CrossRef]
26. Rives, V. (Ed.) *Layered Double Hydroxides: Present and Future*; Nova Science Publishers Inc.: Hauppauge, NY, USA, 2001; ISBN 1590330609.
27. McCullagh, E.; Rigas, N.C.; Gleaves, J.T.; Hodnett, B.K. Selective oxidation of butan-2-one to diacetyl over vanadium pentoxide. An investigation by temporal analysis of products. *Appl. Catal. A Gen.* **1993**, *95*, 183–195. [CrossRef]
28. McCullagh, E.; McMonagle, J.B.; Hodnett, B.K. Kinetic study of the selective oxidation of butan-2-one to diacetyl over vanadium phosphorus oxide. *Appl. Catal. A Gen.* **1993**, *93*, 203–217. [CrossRef]
29. Santos, V.P.; Carabineiro, S.A.C.; Tavares, P.B.; Pereira, M.F.R.; Órfão, J.J.M.; Figueiredo, J.L. Oxidation of CO, ethanol and toluene over TiO_2 supported noble metal catalysts. *Appl. Catal. B Environ.* **2010**, *99*, 198–205. [CrossRef]
30. Lahousse, C.; Bernier, A.; Grange, P.; Delmon, B.; Papaefthimiou, P.; Ioannides, T.; Verykios, X. Evaluation of γ-MnO_2 as a VOC removal catalyst: Comparison with a noble metal catalyst. *J. Catal.* **1998**, *178*, 214–225. [CrossRef]
31. Beauchet, R.; Mijoin, J.; Batonneau-Gener, I.; Magnoux, P. Catalytic oxidation of VOCs on NaX zeolite: Mixture effect with isopropanol and o-xylene. *Appl. Catal. B Environ.* **2010**, *100*, 91–96. [CrossRef]
32. Beauchet, R.; Mijoin, J.; Magnoux, P. Improved catalytic oxidation of cumene by formation of catalytically active species during reaction over NaX zeolite. *Appl. Catal. B Environ.* **2009**, *88*, 106–112. [CrossRef]
33. Lars, S.; Andersson, T. Reaction networks in the catalytic vapor-phase oxidation of toluene and xylenes. *J. Catal.* **1986**, *98*, 138–149. [CrossRef]